ISSN: 1410-8917
Jurnal Kimia Sains & Aplikasi
e-ISSN: 2597-9914

Jurnal Kimia Sains dan Aplikasi 27 (9) (2024): 456-463

Jurnal Kimia Sains dan Aplikasi
Journal of Scientific and Applied Chemistry

Journal homepage: http://ejournal.undip.ac.id/index.php/ksa

Fabrication of Coconut Shell-Derived Graphitic Activated Carbon for Carbon-based Electrode Materials

Irma Fifa Yanti [1], Pratama Jujur Wibawa [1,*], Aris Mukimin [2]

[1] Chemistry Department, Faculty of Sciences and Mathematics, Diponegoro University, Jl. Prof. Soedarto, SH., Tembalang, Semarang, Indonesia
[2] Research Center for Environmental and Clean Technology, National Research and Innovation Agency, BJ Habibie Building 720, Science and Technology Area, Setu, South Tangerang 15314, Indonesia

* Corresponding author: pratamajw@live.undip.ac.id

https://doi.org/10.14710/jksa.27.9.456-463

Article Info

Article history:

Received: 28th July 2024
Revised: 25th September 2024
Accepted: 27th September 2024
Online: 30th September 2024

Keywords:
Coconut shell charcoal; electrode raw material; activated carbon; graphite microstructure

Abstract

This study aims to convert low-value plantation biomass waste into high-value materials. The process involves transforming coconut shell charcoal (CSC) into activated carbon and subsequently producing coconut shell graphitic-like activated carbon (CSGAC). Using a thermal graphitization method with a $FeCl_3$ catalyst at 900°C for 1 hour in a nitrogen atmosphere, graphite microstructures (CSGAC) were formed on the coconut shell activated carbon (CSAC) framework. XRD, FTIR, SEM, and BET analyses confirmed the successful formation of CSGAC. The electrical conductivity of CSGAC, measured at 148 µS, highlights its potential as a cost-effective, renewable, and environmentally friendly raw material for carbon-based electrodes.

1. Introduction

Biomass is a renewable resource widely regarded as a sustainable carbon precursor due to its abundance, low cost, and environmentally friendly nature. The diversity of biomass attracts considerable attention because it offers opportunities for utilization across various applications [1, 2]. Using renewable resources such as biomass is a promising solution, as it can replace carbon materials derived from fossil fuels, whose availability is limited, non-renewable, and unsustainable in the long term [3]. Biomass reduces dependence on fossil carbon sources and provides an effective solution for managing organic waste, such as agricultural or plantation by-products. Organic waste sources include rice husks, coffee grounds [4], coconut shells [5, 6], sugarcane pulp, coconut leaves, and pine bark [7]. Studies have shown that activated carbon derived from coconut shell biomass outperforms other biomass types due to its macroporous structure, which enhances its effectiveness in carbon purification. Consequently, this study selected coconut shells as the carbon source [8].

Activated carbon is recognized as a porous material with a sufficiently large surface area, providing efficient adsorption capabilities and dispersive interactions [6, 9, 10]. It has become a critical component in various applications, including wastewater treatment [9], adsorption of slaughterhouse wastewater [10], methylene blue dye adsorption [11], sensors [12], removal of organic dye pollutants [13], CO_2 capture [14], lithium battery anodes [6], capacitive deionization electrodes [5], cathodes in bioelectrosynthesis cells [15], supercapacitors [8, 16], and gas storage [17].

The versatility of carbon, with its diverse geometric structures, unique properties, electroactivity, stability, excellent electrical conductivity, and high mass density, makes it an ideal candidate for efficient and sustainable electrode materials [3]. In recent decades, significant efforts have been directed toward developing biomass-derived carbon, which offers highly efficient applications in electrochemical storage. Its excellent porosity and surface area enable it to store more electrostatic counterions, thereby enhancing the capacitance (electric double layer) of carbon electrodes [18].

Fossil-based raw materials and metal-containing electrodes face significant limitations, including complex processing and high costs. Additionally, metal-based electrodes are prone to issues such as corrosion and metal ion contamination, further increasing long-term

operational costs and challenges. In contrast, carbon-based electrodes derived from renewable biomass offer more affordable processing and operational benefits [19]. Utilizing carbon from biomass, such as coconut shells, reduces dependence on inorganic electrode materials that contain rare, non-renewable metals. This approach also supports the recycling of biomass waste into high-value products, making it a more cost-effective and environmentally friendly solution [20].

There are significant challenges in using biomass-derived carbon, particularly in controlling the pore structure and optimizing the graphite content—both of which are crucial for enhancing material performance, especially in electrochemical applications [2]. Previous studies have shown that the amorphous structure of activated carbon limits its applications by restricting molecular diffusion, resulting in poor electrochemical properties, such as low conductivity, stability, and irregular pore structures [16, 21].

Therefore, one of the main approaches in this research is to prepare functional electrodes from coconut shell biomass by converting and exploring the structure of coconut shell-activated carbon through graphitization, a method that has not been extensively investigated. The graphitization process aims to produce carbon materials with a high degree of graphitization, crystallinity, and fast diffusion kinetics, ultimately enhancing the performance of the raw electrode materials [18, 22].

This work reports the fabrication of graphite-like microstructures from the activated carbon framework of coconut shells for use as carbon electrode materials. The fabricated materials were characterized and analyzed using several techniques: X-ray diffraction (XRD) to assess the material's crystallinity, Fourier-transform infrared spectroscopy (FTIR) to identify functional groups formed during fabrication, scanning electron microscopy (SEM) to examine surface morphology, Brunauer-Emmett-Teller (BET) nitrogen adsorption to evaluate surface area and pore volume, and conductivity testing to determine the material's potential for electrical conductivity as an electrode.

2. Experimental

2.1. Materials

Coconut shell charcoal (local commercial, Indonesia), sodium hydroxide (NaOH) (Merck, Germany), hydrochloric acid (HCl) (Merck, Germany), distilled water, nitrogen gas (N_2) (99.98%, Samator, Indonesia), iron (III) chloride hexahydrate ($FeCl_3.6H_2O$) (Merck, Germany), and hydrochloric acid (HCl) (Merck, Germany).

2.2. Tools

Commonly available laboratory glassware, such as beakers and volumetric flasks (Pyrex), hot plate stirrer (IKA, Malaysia), electric oven (Memmert, Germany), ball milling machine (Recht PM 200, China), tubular furnace (Carbolite Gero, Germany), X-ray diffraction (XRD) (SHIMADZU XRD-7000 with Cu Kα radiation, λ = 1.54178 Å, Japan), Fourier-transform infrared spectroscopy (FTIR) (Perkin-Elmer, USA), ultraviolet-visible spectrophotometer (UV-Vis) (GENESYS 10S, Japan), scanning electron microscope (SEM) (JEOL JSM-6510LA, Japan), Brunauer-Emmett-Teller (BET) nitrogen gas analyzer (Quantachrome NOVA Win, Japan), and digital electrical conductivity meter (senZ trans, 0-1,999 µS, Singapore).

2.3. Coconut Shell Activated Carbon (CSAC) Fabrication

The fabrication of coconut shell activated carbon (CSAC) was based on previous research, with modifications made as necessary [23, 24]. First, 100 grams of coconut shell charcoal (CSC) were crushed using a blender, followed by ball milling, and then sieved through a 100-mesh sieve to obtain fine coconut shell powder. Next, 50 grams of this fine powder were added to 250 mL of 0.5 M NaOH solution, stirred with a magnetic stirrer on a hotplate at 80°C for 2 hours, and left at room temperature for 24 hours. The mixture was then dried in an oven at 110°C for 12 hours. The following day, the carbon was thermally activated in a tubular furnace at 900°C under a nitrogen atmosphere for 1 hour. After the activation process, the carbon was left to cool overnight in the furnace under a continuous nitrogen gas flow. The following day, the carbon was washed with distilled water until it reached a neutral pH and dried again in the electric oven at 110°C for 12 hours, yielding CSAC as the final product.

2.4. Coconut Shell Graphitic-Like Activated Carbon (CSGAC) Fabrication

The fabrication of coconut shell graphite-like activated carbon (CSGAC) involved several steps, as outlined in references [13, 14, 25]. First, 8 grams of fine CSAC powder were added to 50 mL of 3 M $FeCl_3$ solution and stirred slowly using a magnetic stirrer on a hotplate at 80°C for 2 hours. The carbon and $FeCl_3$ mixture were then dried in an oven at 110°C for 24 hours. The following day, the graphitization process was performed by placing the carbon mixture in a tubular furnace at 900°C under a nitrogen atmosphere with a pressure of 45 kgf/cm², maintained for 1 hour.

After the graphitization, the carbon was left to cool overnight in the furnace while nitrogen gas continued to flow. The next day, the graphitized carbon was rinsed with 2 M HCl solution, followed by distilled water until the pH reached 7. The final product was dried in an electric oven at 80°C for 12 hours, resulting in CSGAC. The overall process for fabricating carbon electrode materials from coconut shells is summarized in Figure 1.

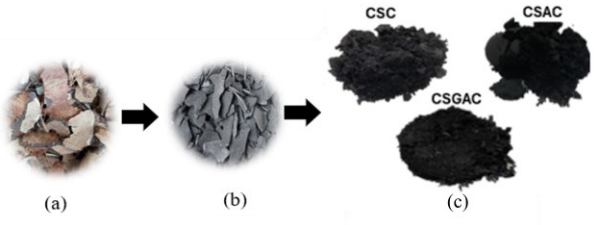

Figure 1. (a) Coconut shell, (b) Coconut shell charcoal/CSC, and (c) CSC, CSAC, CSGAC powder

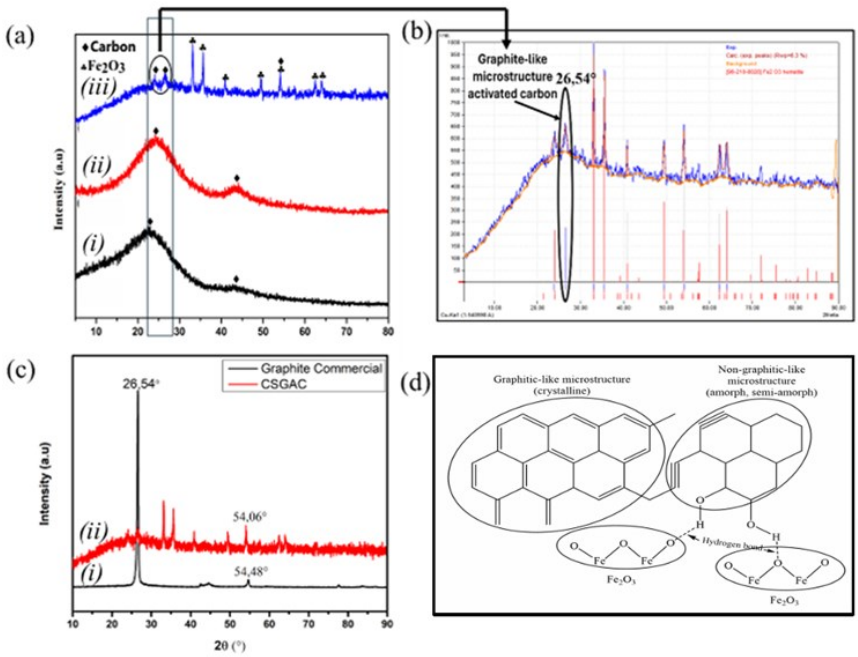

Figure 2. XRD diffractogram of (a)(i) CSC, (ii) CSAC, (iii) CSGAC), (b) CGSAC spectra analyzed by Match software, (c) (ii) XRD diffractogram of CSGAC paired with (i) commercial graphite, and (d) schematic illustration of the carbon framework structure of graphite according to its XRD and FTIR spectra

2.5. Analysis and Characterization

The CSAC and CSC samples were characterized using various analytical techniques to assess crystallinity, functional groups, surface morphology, and porosity. XRD analysis was conducted within the range of $5° \leq 2\theta \leq 90°$, using Cu Kα radiation (λ = 1.5418 Å). This technique provided insights into the crystal phase, crystal structure, lattice parameters, and crystallite size. Diffractogram patterns were analyzed using Match software version 4.0. FTIR analysis was employed to identify functional groups present in the samples, with spectra collected in transmission mode over the range of 400 to 4000 cm^{-1} from KBr pressed pellets. SEM analysis was used to observe the surface morphology of the samples, and particle size distribution was analyzed using ImageJ software. Specific surface area, pore volume, and pore size of the carbon samples were determined through BET analysis, which involved nitrogen adsorption at 77 K under a gas pressure of 757.906 mmHg.

3. Results and Discussion

3.1. X-ray Diffraction (XRD) Analysis

The first characterization performed was determining the crystal structure of the fabricated CSC, CSAC, and CSGAC. XRD testing was conducted, and the results are presented in Figure 2. Figure 2(a) presents the diffractogram patterns of CSC (i) and CSAC (ii), which are very similar, displaying scattering angles (2θ) of approximately 22-24° and 42-45°. These peaks indicate the characteristic amorphous carbon structure [26]. In contrast, the CSGAC diffractogram (iii) exhibits a distinctly different pattern from that of CSC and CSAC. As shown in Figure 2(a)(iii), the CSAC material features sharp peaks of low intensity, with the most notable peaks occurring in the range of $2\theta = 22–28°$.

An in-depth analysis of the diffractogram was conducted using Match 4.0 software, as illustrated in Figure 2(b). In addition to the peaks corresponding to graphite domains, diffraction peaks indicative of hematite compounds (Fe_2O_3) were also detected. The formation of hematite likely occurs during the catalytic graphitization process involving the $FeCl_3$ precursor, which reacts with hydrated H_2O during heating. Fe_2O_3 acts as a catalyst for carbon formation, allowing the carbon precursor to diffuse to the catalyst surface. High temperatures cause the carbon adsorbed on Fe_2O_3 to transform into more organized carbon structures through the formation of Fe_3C carbide.

The Fe_3C compound is metastable and tends to decompose at elevated temperatures (>600°C), becoming unstable and decomposing into iron (Fe) and carbon (C), which leads to the formation of graphite layers. In many cases, metal catalysts or metal oxide residues remain trapped between the graphite layers [17, 27]. This is consistent with the XRD analysis, which shows that the formed CSGAC produces Fe_2O_3 in situ, observable at peaks of 2θ = 24.12°, 33.15°, 35.64°, 40.89°, 49.43°, 54.06°, 57.59°, and 62.49°. The formation of carbon, indicated by two sharp peaks of low intensity in Figure 2(a)(iii), was further analyzed by comparing it with a commercial graphite diffractogram, as shown in Figure 2(c)(i). The results revealed peaks corresponding to CSGAC (Figure 2(c)(ii)) precisely at 2θ = 26.54° and 54.48°, confirming the presence of a graphite microstructure in the CSGAC material.

Quantitative confirmation of the carbon plane analysis was conducted using Bragg's Law, expressed as $n\lambda = 2d_{hkl} \sin \theta$, where n is the diffraction order, λ is the wavelength of the X-rays, d_{hkl} is the distance between the planes, and θ is the angle between the incoming X-rays and their reflections, as detailed in Table 1.

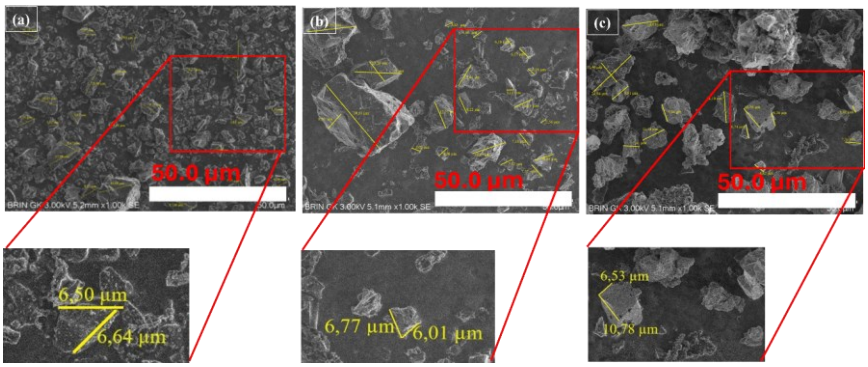

Figure 3. Surface morphologies of (a) CSC, (b) CSAC, and (c) CSGAC

Table 1. Representative distances between planes (d_{hkl}) for each 2θ value of CSC, CSAC, and CSGAC

Sample	hkl	2θ (°)	Distance between planes (Å)
CSC	(002)	23.29	3.81
	(100)	43.4	2.09
CSAC	(002)	24.2	3.67
	(100)	43.4	2.08
CSGAC	(002)	26.54	3.35
	(100)	54.06	1.69

The decrease in the interplane distance (d_{hkl}) of carbon (002) from 3.81 Å in CSC to 3.35 Å in CSGAC indicates an enhancement in structural order, resulting in a denser atomic arrangement. This reduction in interplane distance can be attributed to the intercalation process, which modifies the carbon framework and leads to new properties, such as an increased surface area compared to CSC and CSAC [28]. The measured distance of 3.35 Å in CSGAC confirms the presence of a graphite microstructure, aligning with the d_{hkl} values typically found in commercial graphite, as noted by Vlahov [29].

Furthermore, the presence of Fe_2O_3 molecules within the CSGAC carbon framework enhances material properties and electrical conductivity. This process facilitates a more orderly arrangement of the carbon surface, thereby increasing the volume fraction of crystals within the carbon framework, which significantly enhances conductivity [30]. Consequently, the CSGAC material demonstrates strong potential for good conductivity and can be utilized as a raw material for electrodes.

3.2. Morphological Analysis

The surface morphology of CSC, CSAC, and CSGAC was characterized using an SEM at a magnification of 1000×. The SEM images in Figure 3 illustrate the detailed morphology of each sample. The morphologies of CSC, CSAC, and CSGAC exhibit consistent irregular shapes characteristic of amorphous carbon surfaces. Image J software was utilized to analyze particle size, focusing on one particle from each sample with identical dimensions, resulting in a particle size range of approximately 50 ± 6 µm. The CSC material shown in Figure 3(a) displays a significantly heterogeneous surface morphology, with its irregular features indicating the retention of many natural characteristics of coconut shells.

Table 2. BET analysis results for CSC, CSAC, and CSGAC

Sample	Surface area (m^2/g)	Total pore volume (cm^3/g)	Pore size (nm)
CSC	20.628	0.034	3.342
CSAC	57.924	0.070	2.429
CSGAC	329.603	0.275	3.334

In contrast, the morphology of the CSAC material (Figure 3(b)), which has undergone chemical and physical activation processes, presents a smoother surface. This change may be attributed to the decomposition of volatile organic compounds during carbon purification, resulting in a reduction in small particle sizes and a more uniform distribution of medium to large particles. The next-generation fabrication, CSGAC, shown in Figure 3(c), also exhibits a consistent irregular shape; however, its surface appears smoother than that of CSC and CSAC. This smooth yet dense surface suggests a transition toward a graphitic structure [31]. The differences in structural morphology among CSC, CSAC, and CSGAC are further highlighted by measuring the specific surface area using BET analysis, as presented in Table 2.

The BET analysis of CSC, CSAC, and CSGAC provides quantitative data on the surface characteristics of the materials, complementing the observations from the SEM morphology. As shown in Table 2, the transformation of CSAC) into CSGAC resulted in a significant increase in surface area and pore volume while the pore size decreased. According to Gai *et al.* [2], the specific surface area directly influences particle size; however, particle size does not solely represent surface properties. This phenomenon can be attributed to the destruction of biomass by the iron catalyst, which generates defects in the carbon surface pores.

Research by Dubey *et al.* [3] showed that increased surface area and pore volume in carbon-based materials enhance their potential for energy storage, such as electrodes. CSGAC, as shown in Table 2, has a pore volume of 0.275 cm^3/g and a pore size of 3.334 nm, indicating mesoporous material formation. Similarly, Szczęśniak *et al.* [32] reported analogous results, where the successful formation of mesoporous carbon was linked to an increase in mesopore volume (with pore sizes ranging from 2 to 50 nm) during catalytic graphitization using $FeCl_3$ at 900°C, resulting in a surface area of 347 m^2/g and a pore volume of 0.29 cm^3/g.

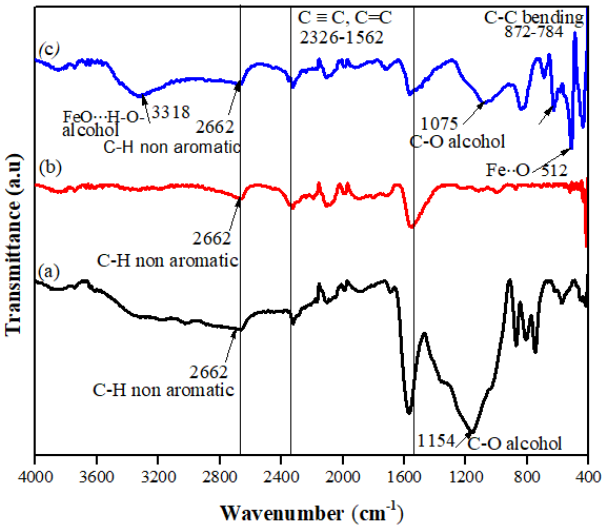

Figure 4. FTIR spectra of (a) CSC, (b) CSAC, and (c) CSGAC

Additionally, Ntakirutimana *et al.* [33] highlighted that activated carbon-based materials with mesoporous surfaces promote enhanced interconnection structures within the electrode matrix. This configuration contributes to increased ionic conductivity by providing efficient pathways for rapid ion transport within the matrix. Therefore, developing carbon-based electrodes with precisely controlled amounts of mesopores and micropores represents a vital strategy for optimizing electrode materials [33]. Given this context, the CSGAC material, with its graphite microstructure framework similar to activated carbon, demonstrates promising conductivity values, positioning it as a suitable candidate for electrode raw materials.

3.3. Fourier Transform Infrared Analysis (FTIR)

The FTIR spectra of CSC, CSAC, and CSGAC provide important information regarding the functional groups present on the carbon surface, as illustrated in Figure 4. Based on the FTIR spectra presented in Figure 4, several peaks are observed at specific wave numbers: 3300 cm^{-1}, 2662 cm^{-1}, 2324-2100 cm^{-1}, 1500 cm^{-1}, 1100 cm^{-1}, 872-690 cm^{-1}, 628 cm^{-1}, and 512 cm^{-1}. This spectrum indicates that the microstructure of coconut shell-activated carbon, which resembles graphite, contains various functional groups. Notably, a narrow peak around 3318 cm^{-1} shows the stretching vibration of unbound OH [34]. Other groups include aliphatic chains (CH), alkenyl C≡C, C=C, CO, CH out of the plane, and stretching vibrations of FeO. A complete summary of the FTIR spectrum peaks is shown in Figure 4, summarized in Table 3.

Based on the identified functional groups on the surface of the synthesized carbon, the CSGAC, which serves as the target material, exhibits a carbon framework comprising sp^3 (saturated carbon atoms), sp^2 (non-aromatic unsaturated carbon atoms), and sp (unsaturated carbon atoms) hybridization of the carbon atom orbitals. This information is crucial for evaluating the electrochemical properties of the material, particularly in terms of its conductivity as a potential electrode preparation material.

Table 3. Summarized functional group representation of CSC, CSAC, and CSGAC

No.	Wavenumber (cm^{-1})	Functional group analysis	References
1	3318	v(OH) bond	[34]
2	2662	Saturated, v(CH)	[35]
3	2326-2102	Unsaturated, v(C≡C)	[36, 37]
4	1569-1552	Unsaturated hexagonal ring, v(C=C)	[38]
5	1154-1075	Alcohol v(C–O)	[23, 24]
6	827-748	Out of plane, v(CH)	[39]
7	625	Saturated, v(CC)	[40]
8	512	α-Fe_2O_3, v(Fe-O)	[41]

3.4. Conductivity Analysis

Conductivity testing was conducted on CSC, CSAC, and CSGAC samples to assess their electrical conductivity, which is a critical property for their application as electrode materials. The conductivity of the carbon material electrodes, as shown in Table 4, indicates a progression from CSC to a graphite microstructure (CSGAC) in the order of CSC < CSAC < CSGAC. This trend highlights the transformation of the amorphous structure of coconut shell charcoal into a more organized graphite microstructure, which significantly enhances conductivity. The improvement in conductivity can be attributed to the more regular carbon framework structure of CSGAC, resulting in a 97.33% increase in conductivity compared to CSC.

The conductivity analysis of the CSGAC material, alongside XRD, SEM, BET, and FTIR characterizations, reveals a stronger correlation with the enhanced conductivity when compared to CSC and CSAC. The carbon structure of CSGAC consists of a mixture of sp^3 and sp^2 hybridization bonds, which is crucial for its conductivity properties. In the graphite structure, each carbon atom possesses four valence electrons: three participate in forming sp^2 hybridization with sigma (σ) covalent bonds, while the fourth engages in pi (π) covalent bonding. These π electrons create a conjugated system that can move freely across the graphite-like microstructure, enabling CSGAC to generate an electric current when exposed to electrical energy [8, 42].

Furthermore, the analysis of carbon surface morphology (Section 3.2) indicates that the mesoporous nature of CSGAC facilitates the transport of molecules and ions, thereby enhancing conductivity. The mobility of π electrons allows for free movement throughout the CSGAC surface, including through the Fe_2O_3 trapped within it. Although Fe_2O_3 has low conductivity (10^{-10} S/cm) [30], its presence in Fe_2O_3/carbon composites has been shown to enhance electrochemical properties and improve conductivity compared to the individual materials [43].

Table 4. Conductivity of CSC and CSAC materials

Sample	Conductivity (µS)
CSC	75
CSAC	95
CSGAC	148

For instance, Irdhawati *et al.* [44] reported the use of Fe_2O_3 as an alloy material in carbon paste electrodes for dopamine measurement. The inclusion of Fe_2O_3 accelerates electron transfer rates and creates gaps between graphite layers on the electrode surface, positively impacting the electrocatalytic efficiency of the electrode. Thus, CSGAC material, with its combination of graphite and Fe_2O_3 microstructures, emerges as a promising candidate for better electrode material preparation compared to CSC and CSAC.

According to Zhang *et al.* [45], the conductivity of natural graphite varies with impurity levels and exhibits anisotropic properties. For pure graphite sheets, the through-plane conductivity ranges from 3 S/cm to 25 S/cm, while the in-plane conductivity varies significantly, ranging from 500 S/cm to 1700 S/cm. Frattini *et al.* [46] reported the use of 4.5 µm graphite to prepare a conductive material with a conductivity of 2 S/m. By varying the mass fraction of graphite, the conductivity of the mixture increased from 10^{-5} S/m to 1 S/m. In contrast, commercial graphitic carbon reported by Vilar *et al.* [47] has a conductivity value of 110 µS.

In this study, the synthesized graphite material (CSGAC) obtained from biomass carbon demonstrated a conductivity of 148 µS, highlighting its advantages over existing materials. Based on the findings from several studies, the CSGAC material shows potential as an alternative electrode material that is cost-effective, easily accessible, renewable, and environmentally friendly.

4. Conclusion

The production of coconut shell-activated carbon graphite was successfully achieved using the thermal graphitization catalyst method. This process utilizes thermal energy to transform a portion of the carbon molecular framework from an irregular arrangement to a more organized structure, resulting in a graphite-like microstructure. This structure contains Fe_2O_3, which is produced in situ from the $FeCl_3$ catalyst precursor during the heating process. Coconut shell graphitic-like activated carbon (CSGAC) has shown potential as a cost-effective and renewable carbon-based electrode material, exhibiting a conductivity of 148 µS.

Acknowledgment

The author would like to thank the ORNM Program of the National Research and Innovation Agency for their financial support under the research budget scheme No. 2059/HK.01.00/4/2023.

References

[1] Jiang Deng, Mingming Li, Yong Wang, Biomass-derived carbon: synthesis and applications in energy storage and conversion, *Green Chemistry*, 18, 18, (2016), 4824-4854 https://doi.org/10.1039/c6gc01172a

[2] Lili Gai, Jianbin Li, Qi Wang, Run Tian, Kai Li, Evolution of biomass to porous graphite carbon by catalytic graphitization, *Journal of Environmental Chemical Engineering*, 9, 6, (2021), 106678 https://doi.org/10.1016/j.jece.2021.106678

[3] Prashant Dubey, Vishal Shrivastav, Priyanka H. Maheshwari, Shashank Sundriyal, Recent advances in biomass derived activated carbon electrodes for hybrid electrochemical capacitor applications: Challenges and opportunities, *Carbon*, 170, (2020), 1-29 https://doi.org/10.1016/j.carbon.2020.07.056

[4] Marcela Paredes-Laverde, Maurin Salamanca, Javier Silva-Agredo, Lis Manrique-Losada, Ricardo A. Torres-Palma, Selective removal of acetaminophen in urine with activated carbons from rice (*Oryza sativa*) and coffee (*Coffea arabica*) husk: Effect of activating agent, activation temperature and analysis of physical-chemical interactions, *Journal of Environmental Chemical Engineering*, 7, 5, (2019), 103318 https://doi.org/10.1016/j.jece.2019.103318

[5] Le Thanh Nguyen Huynh, Thi Nam Pham, Thai Hoang Nguyen, Viet Hai Le, Thi Thom Nguyen, Thi Diem Kieu Nguyen, Thanh Nhut Tran, Pham Anh Vu Ho, Thanh Thien Co, Thi Thu Trang Nguyen, Thi Kieu Anh Vo, Trung Huy Nguyen, Thi Thu Vu, Viet Mui Luong, Hiroshi Uyama, Gia Vu Pham, Thai Hoang, Dai Lam Tran, Coconut shell-derived activated carbon and carbon nanotubes composite: a promising candidate for capacitive deionization electrode, *Synthetic Metals*, 265, (2020), 116415 https://doi.org/10.1016/j.synthmet.2020.116415

[6] Daisuke Higai, Zhebin Huang, Eika W. Qian, Preparation and surface characteristics of phosphoric acid-activated carbon from coconut shell in air, *Environmental Progress & Sustainable Energy*, 40, 2, (2021), e13509 https://doi.org/10.1002/ep.13509

[7] K. Malini, D. Selvakumar, N. S. Kumar, Activated carbon from biomass: Preparation, factors improving basicity and surface properties for enhanced CO_2 capture capacity – A review, *Journal of CO_2 Utilization*, 67, (2023), 102318 https://doi.org/10.1016/j.jcou.2022.102318

[8] Rabi Kabir Ahmad, Shaharin Anwar Sulaiman, Suzana Yusup, Sharul Sham Dol, Muddasser Inayat, Hadiza Aminu Umar, Exploring the potential of coconut shell biomass for charcoal production, *Ain Shams Engineering Journal*, 13, 1, (2022), 101499 https://doi.org/10.1016/j.asej.2021.05.013

[9] Zhihua Deng, Shixian Sun, Huijuan Li, Duo Pan, Rahul Rangrao Patil, Zhanhu Guo, Ilwoo Seok, Modification of coconut shell-based activated carbon and purification of wastewater, *Advanced Composites and Hybrid Materials*, 4, (2021), 65-73 https://doi.org/10.1007/s42114-021-00205-4

[10] Ibrahim Mohammed Lawal, Usman Bala Soja, Abdulhameed Danjuma Mambo, Shamsul Rahman Mohamed Kutty, Ahmad Hussaini Jagaba, Gasim Hayder, Sule Abubakar, Ibrahim Umaru, Adsorption

of Abattoir Wastewater Contaminants by Coconut Shell-Activated Carbon, *Sustainability Challenges and Delivering Practical Engineering Solutions*, Cham, 2023 https://doi.org/10.1007/978-3-031-26580-8_22

[11] Hatice Karaer Yağmur, İsmet Kaya, Synthesis and characterization of magnetic $ZnCl_2$-activated carbon produced from coconut shell for the adsorption of methylene blue, *Journal of Molecular Structure*, 1232, (2021), 130071 https://doi.org/10.1016/j.molstruc.2021.130071

[12] Shweta J. Malode, Mahesh M. Shanbhag, Rohini Kumari, Daphika S. Dkhar, Pranjal Chandra, Nagaraj P. Shetti, Biomass-derived carbon nanomaterials for sensor applications, *Journal of Pharmaceutical and Biomedical Analysis*, 222, (2023), 115102 https://doi.org/10.1016/j.jpba.2022.115102

[13] Seyedehmaryam Moosavi, Chin Wei Lai, Sinyee Gan, Golnoush Zamiri, Omid Akbarzadeh Pivehzhani, Mohd Rafie Johan, Application of Efficient Magnetic Particles and Activated Carbon for Dye Removal from Wastewater, *ACS Omega*, 5, 33, (2020), 20684-20697 https://doi.org/10.1021/acsomega.0c01905

[14] Xiuli Li, Mingyang Gu, Feng Zhang, Qingwang Min, Lifeng Chen, Effects of raw materials on the structures of three dimensional graphene/amorphous carbon composites derived from biomass resources, *Research on Chemical Intermediates*, 45, 3, (2019), 1131-1145 https://doi.org/10.1007/s11164-018-3669-5

[15] Aris Mukimin, Rustiana Yuliasni, Nur Zen, Kukuh Wicaksono, Januar Arif Fatkhurahman, Hanny Vistanty, Rizal Awaludin Malik, Synthesis of Graphite Porous Electrode Based on Coconut Shell as a Potential Cathode in Bioelectrosyntesis Cell, *Indonesian Journal of Chemistry*, 19, 2, (2019), 413-421 https://doi.org/10.22146/ijc.37550

[16] Azrine Ajien, Juferi Idris, Nurzawani Md Sofwan, Rafidah Husen, Hazman Seli, Coconut shell and husk biochar: A review of production and activation technology, economic, financial aspect and application, *Waste Management & Research*, 41, 1, (2023), 37-51 https://doi.org/10.1177/0734242x221127167

[17] Radosław Tarkowski, Barbara Uliasz-Misiak, Piotr Tarkowski, Storage of hydrogen, natural gas, and carbon dioxide – Geological and legal conditions, *International Journal of Hydrogen Energy*, 46, 38, (2021), 20010-20022 https://doi.org/10.1016/j.ijhydene.2021.03.131

[18] Suresh Sagadevan, Thivyah Balakrishnan, Md Zillur Rahman, Tetsuo Soga, Hyacinthe Randriamahazaka, Babak Kakavandi, Mohd Rafie Johan, Agricultural biomass-based activated carbons for efficient and sustainable supercapacitors, *Journal of Energy Storage*, 97, (2024), 112878 https://doi.org/10.1016/j.est.2024.112878

[19] Chuan Yuan, Hao Xu, Sherif A. El-khodary, Guosong Ni, Sivakumar Esakkimuthu, Shan Zhong, Shuang Wang, Recent advances and challenges in biomass-derived carbon materials for supercapacitors: A review, *Fuel*, 362, (2024), 130795 https://doi.org/10.1016/j.fuel.2023.130795

[20] Tilahun Temesgen, Eneyew Tilahun Bekele, Bedasa Abdisa Gonfa, Lemma Teshome Tufa, Fedlu Kedir Sabir, Sisay Tadesse, Yilkal Dessie, Advancements in biomass derived porous carbon materials and their surface influence effect on electrode electrochemical performance for sustainable supercapacitors: A review, *Journal of Energy Storage*, 73, (2023), 109293 https://doi.org/10.1016/j.est.2023.109293

[21] Kalu Samuel Ukanwa, Kumar Patchigolla, Ruben Sakrabani, Edward Anthony, Sachin Mandavgane, A Review of Chemicals to Produce Activated Carbon from Agricultural Waste Biomass, *Sustainability*, 11, 22, (2019), 6204 https://doi.org/10.3390/su11226204

[22] Xiaohua Zhang, Ruyun Han, Yanzhen Liu, Hengxiang Li, Wenjing Shi, Xiaoyan Yan, Xinxin Zhao, Yongfeng Li, Baosheng Liu, Porous and graphitic structure optimization of biomass-based carbon materials from 0D to 3D for supercapacitors: A review, *Chemical Engineering Journal*, 460, (2023), 141607 https://doi.org/10.1016/j.cej.2023.141607

[23] Badreddine Belhamdi, Hamza Laksaci, Chemseddine Belabed, Zoulikha Merzougui, Salim Boudiaf, Rachid Tir, Mohamed Trari, Synthesis of highly porous activated carbon derived from kernel oil treatment by-products of Argania Spinosa as a recyclable adsorbent for amoxicillin removal from real wastewater, *Biomass Conversion and Biorefinery*, 13, 3, (2023), 2135-2149 https://doi.org/10.1007/s13399-021-01380-6

[24] Nguyen Van Hung, Bui Thi Minh Nguyet, Nguyen Huu Nghi, Nguyen Mau Thanh, Nguyen Duc Vu Quyen, Vo Thang Nguyen, Dao Ngoc Nhiem, Dihn Quang Khieu, Highly effective adsorption of organic dyes from aqueous solutions on longan seed-derived activated carbon, *Environmental Engineering Research*, 28, 3, (2023), 220116-220110 https://doi.org/10.4491/eer.2022.116

[25] Patrick T. Moseley, David A. J. Rand, Alistair Davidson, Boris Monahov, Understanding the functions of carbon in the negative active-mass of the lead–acid battery: A review of progress, *Journal of Energy Storage*, 19, (2018), 272-290 https://doi.org/10.1016/j.est.2018.08.003

[26] Pratama Jujur Wibawa, Muhammad Nur, Mukhamad Asy'ari, Hadi Nur, SEM, XRD and FTIR analyses of both ultrasonic and heat generated activated carbon black microstructures, *Heliyon*, 6, 3, (2020), e03546 https://doi.org/10.1016/j.heliyon.2020.e03546

[27] Yedluri Anil Kumar, Ganesh Koyyada, Tholkappiyan Ramachandran, Jae Hong Kim, Sajid Sajid, Md Moniruzzaman, Salem Alzahmi, Ihab M. Obaidat, Carbon Materials as a Conductive Skeleton for Supercapacitor Electrode Applications: A Review, *Nanomaterials*, 13, 6, (2023), 1049 https://doi.org/10.3390/nano13061049

[28] Sang-Min Lee, Sang-Hye Lee, Jae-Seung Roh, Analysis of Activation Process of Carbon Black Based on Structural Parameters Obtained by XRD Analysis, *Crystals*, 11, 2, (2021), 153 https://doi.org/10.3390/cryst11020153

[29] Alexander Vlahov, XRD graphitization degrees: a review of the published data and new calculations, correlations, and applications, *Geologica Balcanica*, 50, 1, (2021), 11-35 https://doi.org/10.52321/GeolBalc.50.1.11

[30] Zhaoxia Song, Wei Liu, Wensuo Wei, Chengze Quan, Nanxuan Sun, Quan Zhou, Guichang Liu, Xiaoqiong Wen, Preparation and electrochemical properties of Fe_2O_3/reduced graphene oxide aerogel (Fe_2O_3/rGOA) composites for supercapacitors, *Journal of Alloys and Compounds*, 685, (2016), 355-363 https://doi.org/10.1016/j.jallcom.2016.05.323

[31] Jiyeol Bae, Suho Kim, Soyoung Baek, Parallelly Aligned, Activated Carbon Coated Plates Operating as Adsorption Columns for Removing VOCs, *Aerosol and Air Quality Research*, 22, 3, (2022), 210263 https://doi.org/10.4209/aaqr.210263

[32] Barbara Szczęśniak, Jerzy Choma, Mietek Jaroniec, Sustainable mechanochemical synthesis of catalytically graphitized mesoporous carbons, *Microporous and Mesoporous Materials*, 372, (2024), 113117 https://doi.org/10.1016/j.micromeso.2024.113117

[33] Samuel Ntakirutimana, Wei Tan, Marc A. Anderson, Yang Wang, Editors' Choice—Review—Activated Carbon Electrode Design: Engineering Tradeoff with Respect to Capacitive Deionization Performance, *Journal of The Electrochemical Society*, 167, 14, (2020), 143501 https://doi.org/10.1149/1945-7111/abbfd7

[34] Yufeng Zhao, Chul-Woong Cho, Longzhe Cui, Wei Wei, Junxiong Cai, Guiping Wu, Yeoung-Sang Yun, Adsorptive removal of endocrine-disrupting compounds and a pharmaceutical using activated charcoal from aqueous solution: kinetics, equilibrium, and mechanism studies, *Environmental Science and Pollution Research*, 26, 33, (2019), 33897-33905 https://doi.org/10.1007/s11356-018-2617-7

[35] Tang Shu Hui, Muhammad Abbas Ahmad Zaini, Valorization of spent activated carbon in glycerine deodorization unit for methylene blue removal, *Carbon Letters*, 31, 4, (2021), 721-728 https://doi.org/10.1007/s42823-020-00189-z

[36] Ali Mohammed Saleh, Hadi Hamdi Mahdi, Azil Bahari Alias, Nurul Kairiah Abd Hadi, Deana Qarizada, Ali H. Jawad, Noah Mohammed Saleh, Equilibrium and kinetic studies in adsorption of H_2S using coconut shell activated carbon xerogel: Effect of mass adsorbent and temperature, *Desalination and Water Treatment*, 317, (2024), 100149 https://doi.org/10.1016/j.dwt.2024.100149

[37] Bishnu P. Thapaliya, Huimin Luo, Phillip Halstenberg, Harry M. Meyer III, John R. Dunlap, Sheng Dai, Low-Cost Transformation of Biomass-Derived Carbon to High-Performing Nano-graphite via Low-Temperature Electrochemical Graphitization, *ACS Applied Materials & Interfaces*, 13, 3, (2021), 4393-4401 https://doi.org/10.1021/acsami.0c19395

[38] Benjamin Diby Ossonon, Daniel Bélanger, Synthesis and characterization of sulfophenyl-functionalized reduced graphene oxide sheets, *RSC Advances*, 7, 44, (2017), 27224-27234 https://doi.org/10.1039/c6ra28311j

[39] John Coates, Interpretation of Infrared Spectra, A Practical Approach, in: *Encyclopedia of Analytical Chemistry*, John Wiley & Sons, Ltd., 2006, https://doi.org/10.1002/9780470027318.a5606

[40] Saeedeh Hashemian, Khaterah Salari, Hamila Salehifar, Zahra Atashi Yazdi, Removal of Azo Dyes (Violet B and Violet 5R) from Aqueous Solution Using New Activated Carbon Developed from Orange Peel, *Journal of Chemistry*, 2013, 1, (2013), 283274 https://doi.org/10.1155/2013/283274

[41] Lufei Yang, Zhiyuan Mi, Haichao Fang, Ruizhe Xu, Binyang Lv, Jizhen Li, Guofang Zhang, Fabrication of highly catalytic active α -Fe_2O_3-carbon nanotube composites for thermal decomposition of ammonium perchlorate by light and temperature control strategy, *Surfaces and Interfaces*, 44, (2024), 103642 https://doi.org/10.1016/j.surfin.2023.103642

[42] Ruisong Wei, Hongfang Lai, Seyed Mahmoud Mirzamani Bafghi, The Catalysis of Ferric Chloride in the Preparation of Graphene Oxide Film, *Iranian Journal of Chemistry and Chemical Engineering*, 41, 3, (2022), 832-842 https://doi.org/10.30492/ijcce.2021.136138.4326

[43] KaiJie Dong, ZhaoKun Yang, DongJian Shi, MingQing Chen, Weifu Dong, Nitrogen-doped carbon boosting Fe_2O_3 anode performance for supercapacitors, *Journal of Materials Science: Materials in Electronics*, 33, 17, (2022), 13547-13557 https://doi.org/10.1007/s10854-022-08289-4

[44] Irdhawati Irdhawati, Manuntun Manurung, Ni Ketut Yuni Sri Lestari, Preparation and Validation of Fe_2O_3 Modified Carbon Paste Electrode for Measurement of Dopamine by Voltammetry Method, *Jurnal Kimia Sains dan Aplikasi*, 22, 6, (2019), 227-234 https://doi.org/10.14710/jksa.22.6.227-234

[45] Shifan Zhang, Neven Ukrainczyk, Ali Zaoui, Eddie Koenders, Electrical conductivity of geopolymer-graphite composites: Percolation, mesostructure and analytical modeling, *Construction and Building Materials*, 411, (2024), 134536 https://doi.org/10.1016/j.conbuildmat.2023.134536

[46] Domenico Frattini, Grazia Accardo, Claudio Ferone, Raffaele Cioffi, Fabrication and characterization of graphite-cement composites for microbial fuel cells applications, *Materials Research Bulletin*, 88, (2017), 188-199 https://doi.org/10.1016/j.materresbull.2016.12.037

[47] E. O. Vilar, N. L. de Freitas, F. R. de Lirio, FB de Sousa, Study of the electrical conductivity of graphite felt employed as a porous electrode, *Brazilian Journal of Chemical Engineering*, 15, 3, (1998), 295-302 https://doi.org/10.1590/S0104-66321998000300007